REPORT DOCUMENTATION PAGE

Form Approved
OMB No. 0704-0188

1. REPORT DATE *(DD-MM-YYYY)*	2. REPORT TYPE	3. DATES COVERED *(From - To)*
27-02-1998	Paper	

4. TITLE AND SUBTITLE

Aspect Ratio and Loading Effects on a Cracked Rectangular Tension Specimen Made from a Linear Elastic Material

5a. CONTRACT NUMBER

5b. GRANT NUMBER

5c. PROGRAM ELEMENT NUMBER

6. AUTHOR(S)

D.T. Baron[1]; C.T. Liu[2]

5d. PROJECT NUMBER
2303

5e. TASK NUMBER
M2C8

5f. WORK UNIT NUMBER

7. PERFORMING ORGANIZATION NAME(S) AND ADDRESS(ES) AND ADDRESS(ES)

[1]Raytheon STX Corp.
Edwards AFB CA 93524

[2]Air Force Research Laboratory (AFMC)
AFRL/PRS
5 Pollux Drive
Edwards AFB CA 93524-7048

8. PERFORMING ORGANIZATION REPORT

9. SPONSORING / MONITORING AGENCY NAME(S) AND ADDRESS(ES)

Air Force Research Laboratory (AFMC)
AFRL/PRS
5 Pollux Drive
Edwards AFB CA 93524-7048

10. SPONSOR/MONITOR'S ACRONYM(S)

11. SPONSOR/MONITOR'S NUMBER(S)
AFRL-PR-ED-TP-1998-058

12. DISTRIBUTION / AVAILABILITY STATEMENT
Approved for public release; distribution unlimited.

13. SUPPLEMENTARY NOTES

14. ABSTRACT

20020115 066

15. SUBJECT TERMS

16. SECURITY CLASSIFICATION OF:			17. LIMITATION OF ABSTRACT	18. NUMBER OF PAGES	19a. NAME OF RESPONSIBLE PERSON
					C.T. Liu
a. REPORT	b. ABSTRACT	c. THIS PAGE	A		19b. TELEPHONE NUMBER *(include area code)*
Unclassified	Unclassified	Unclassified			(661) 275-5642

ASPECT RATIO AND LOADING EFFECTS ON A CRACKED RECTANGULAR TENSION SPECIMEN MADE FROM A LINEAR ELASTIC MATERIAL

D.T. Baron
Raytheon STX Corp.
Edwards AFB, CA

C.T. Liu
Air Force Research Laboratory
Edwards AFB, CA

ABSTRACT

Finite element calculations are performed to determine the effect of specimen aspect ratio (specimen height (h) divided by specimen width (w)) on the specimen geometry stress intensity correction factor ($F = \sqrt{JE}/(\sigma\sqrt{\pi a})$) (where J is the J-integral, E is Young's modulus, σ is the remote force divided by the uncracked area, and a is the crack length). F is a function of specimen geometry, and modifies the value of the Mode 1 stress intensity (K_1). Linear elastic fracture mechanics (LEFM) and plane stress are assumed. Two specimen types are simulated, center cracked tension (CCT), and single edge notched tension (SENT). Two boundary conditions are simulated, prescribed uniform load, and prescribed uniform displacement. For each of the four combinations of specimen type and boundary condition, an estimate is made of the minimum value of h/w for which the effect on F can be neglected, in which case F can be calculated using an equation instead of from a numerical analysis.

INTRODUCTION

An important problem in engineering design is evaluating the strength and reliability of structures. It is known that the strength of a structure may decrease during the period of its design life under service loads. One of the common causes of weakening is the development of structural cracks. However, the presence of cracks in a structure does not necessarily mean that the structure is no longer functional. Therefore, to calculate the ultimate strength or the maximum service life of a structure, studies are conducted to quantify the significance of flaw types and size, and to determine whether a crack will grow, and the rate of growth. In this study, finite element simulations are performed of two commonly used fracture mechanics test specimens, CCT and SENT (Figure 1). It is important to be able to calculate the Mode 1 stress intensity factors for these specimens for any combinations of boundary condition, specimen aspect ratio (h/w) and crack length to specimen width ratio (a/w). The specimen geometry stress intensity correction factor (F) enables the calculation. For large values of h/w, F is independent of h/w, and formulas exist for F. In this paper, finite element calculations are made to determine how big h/w must be in order to be neglected, and the effect on F for smaller values of h/w.

SPECIMEN GEOMETRY STRESS INTENSITY CORRECTION FACTOR

The specimen geometry stress intensity correction factor, (F), is defined as

$$F(J, E, \sigma, a) \equiv \frac{\sqrt{JE}}{\sigma\sqrt{\pi a}}; \tag{1}$$

where J is the J-integral, E is Young's modulus, σ is the remote force divided by the uncracked area, and a is the

Distribution Statement - Approved for public release; distribution is unlimited.

crack length. F quantifies the effect of specimen geometry on K_1. Equation (1) has the form of a calculated value of K_1 ($\sqrt{JE}$), divided by a reference value of K_1 ($\sigma\sqrt{\pi a}$). If for a particular experimental specimen, F, σ, and a are known, then

$$K_1 = (F)(\sigma\sqrt{\pi a}). \tag{2}$$

This is how F is used, for calculating the values of K_1 for experimental specimens. For any LEFM specimen with a remotely applied load, K_1 can be written in the form [1]

$$K_1 = \frac{P}{b\sqrt{w}} f\left(\frac{a}{w}\right). \tag{3}$$

P is an applied concentrated force, b is the specimen thickness, and w is the specimen width. Each specimen type has a particular function $f(a/w)$. For CCT and SENT specimens, the validity of equation (3) depends on the specimen aspect ratio (h/w) being large enough so that their exists a cross section between P and the crack which is loaded in uniform tension. In that case the particular value of h/w has no effect on the value of K_1. Substituting the identity $P/(b\sqrt{w}) \equiv \sigma\sqrt{w}$ into equation (3) gives

$$K_1 = \sigma\sqrt{w} f\left(\frac{a}{w}\right). \tag{4}$$

Equation (4) can be used with the LEFM relation $J = K_1^2/E$ to transform equation (1) into

$$F\left(\frac{a}{w}\right) = \sqrt{\frac{w}{\pi a}} f\left(\frac{a}{w}\right). \tag{5}$$

Note that equation (5) depends only on the ratio a/w. Geometrically scaling a specimen (multiplying a, h, and w by the same scalar) has no effect on F. Using equation (5) with the function $f(a/w)$ for a CCT specimen [1] gives the CCT specimen correction factor,

$$F_{\text{CCT}} = \sqrt{\sec\left(\frac{\pi a}{2w}\right)}\left[1 - 0.025\left(\frac{a}{w}\right)^2 + 0.06\left(\frac{a}{w}\right)^4\right]. \tag{6}$$

Using equation (5) with the function $f(a/w)$ for a SENT specimen [1] gives the SENT specimen correction factor,

$$F_{\text{SENT}} = \frac{\sqrt{\frac{2w}{\pi a}\tan\left(\frac{\pi a}{2w}\right)}}{\cos\left(\frac{\pi a}{2w}\right)}\left[0.752 + 2.02\left(\frac{a}{w}\right) + 0.37\left\{1 - \sin\left(\frac{\pi a}{2w}\right)\right\}^3\right]. \tag{7}$$

Equations (6) and (7) are the CCT and SENT specimen geometry stress intensity correction factors for large specimen aspect ratios (h/w). The values of F_{CCT} and F_{SENT} can be computed for any valid value of a/w $(0 < a/w < 1)$ using equations (6) and (7). No numerical analysis is required.

NUMERICAL RESULTS

Table 1 shows the values of finite element calculations of the specimen geometry stress intensity correction factor (F). The calculations were made to determine the influence of specimen aspect ratio (h/w) on F for both CCT and SENT specimens. In the table, each simulated specimen is labeled as being of type CCT or SENT. Additionally each specimen has a three character code consisting of an uppercase letter ("L" or "D") and a two digit number. "L" indicates the specimen was subjected to a uniform load, and "D" indcates the specimen was subjected to a uniform displacement. The two digit number is the specimen aspect ratio. For instance, specimen "CCT L14" is a simulated CCT specimen with a prescribed uniform load, and $h/w = 1/4$. There are two exception specimens in Table 1. The correction factors shown for specimen "CCT EQ6" were calculated using equation (6), and those for specimen "SENT EQ7" were calculated using equation (7). No finite element calculations were made for these two specimens. The values of F in the row for specimen "CCT EQ6" are the limiting values for a CCT specimen as h/w increases, and the values of F in the row for specimen "SENT EQ7" have the analogous meaning for SENT specimens. Figures 2-5 were made from the data of Table 1, and are plots of (F) versus a/w for constant h/w. Figures 2 and 3 are for CCT specimens, and Figures 4 and 5 are for SENT specimens. Figures 2 and 4 are for applied uniform load, and Figures 3 and 5 are for applied uniform displacement. The data of Table 1 specimens "CCT L##" and specimen "CCT EQ6" are plotted in Figure 2. The data of Table 1 specimens "CCT D##" and specimen "CCT EQ6" are plotted in Figure 3. The data of Table 1 specimens "SENT L##" and specimen "SENT EQ7" are plotted in Figure 4. The data of Table 1 specimens "SENT D##" and specimen "SENT EQ7" are plotted in Figure 5. Figure 7 plots the same data as Figure 5, but a/w and h/w are switched. Figure 6 shows second order polynomial curve fits of the induced nodal stresses along the tops of specimens "SENT D##" (Figures 5, 7). Curve fit values are shown instead of the actual values because a finite element solution gives actual nodal stress values which oscillate.

Figures 2 and 3 show that for a CCT specimen subjected to either prescribed uniform load or prescribed uniform displacement, the effect of h/w on F can be neglected when $h/w \geq 3$, and equation (6) can be used to calculate F. Figure 4 shows that for a SENT specimen subjected to a prescribed uniform load, the effect of h/w on F can be ignored when $h/w \geq 2$, and equation (7) can be used to calculate F. Figure 5 shows that for a SENT specimen subjected to a prescribed uniform displacement, it is always necessary to include the effect of h/w on F (except when a/w is small (say $a/w \leq 0.10$), and simultaneously h/w is not small (say $h/w \geq 3$)); and therefore it is necessary to perform a numerical analysis in order to obtain the value of F for a particular value of h/w.

Figures 2-5 show the same trends for both specimen types (CCT, SENT). For a specimen with a prescribed uniform load, decreasing the specimen aspect ratio (h/w) increases the correction factor. For a specimen with a prescribed uniform displacement, decreasing the specimen aspect ratio decreases the correction factor. Explanations can be given for these trends. The equation for the correction factor is $F = \sqrt{JE}/(\sigma\sqrt{\pi a})$. For the case of prescribed uniform load (σ is constant) with a crack of fixed length (a is constant), only J can vary. As the specimen aspect ratio decreases, the amount of material between the (constant) applied traction and the crack surface decreases. The remaining material must deform more to carry the same load. This results in a larger crack opening displacement (COD), therefore a larger value for K_1, and consequently a larger value for J, resulting in a larger value for F. For the case of prescribed uniform displacement, as the specimen aspect ratio decreases, the amount of material between the (constant) applied displacement and the crack surface decreases. The resistance of this material to displacement decreases (the material acts like a beam with a shrinking moment of inertia) while the resistance of the material in front of the crack is constant. The induced stress distribution at the top of the specimen rotates so that the stress behind the crack tip decreases with respect to the stress in front of the crack tip. This results in a decrease in the quantity $\sqrt{J}/\sigma$, and therefore a decrease in F. Figure 6 shows the approximate induced stress distributions along the tops of the SENT specimens subjected to a prescribed uniform displacement (specimens "SENT D##"). As the specimen aspect ratio (h/w) decreases, the stress distribution rotates counterclockwise and the crack is unloaded (the crack is on the left side of the specimen). For a CCT specimen, any cross-sectional stress distribution must be

symmetric. This makes the specimen geometry stress intensity correction factor (F) for a CCT specimen subjected to a prescribed uniform displacement much less sensitive than the corresponding SENT specimen, to the effect of specimen aspect ratio (h/w).

In Figure 5 (SENT specimens, prescribed uniform displacement), by increasing h/w above the maximum shown value $(8/1)$, it should be possible to produce an F curve which is arbitrarily close to the (limit) curve of equation (7). In Figure 7 (a re-plot of data from Figure 5), the limiting value for F as h/w increases of (for instance) the curve for $a/w = 0.5$, should be 2.827 (the value of equation (7) when $a/w = 0.5$). By inspection of Figures 5 and 7 it seems that h/w would have to be very large for the effect of h/w on F (especially for large values of a/w) to be negligible.

DETAILS OF FINITE ELEMENT CALCULATIONS

The finite element calculations were made using the ABAQUS commercial finite element program. Every number in Table 1 (except for the rows corresponding to "CCT EQ6" and "SENT EQ7") required one finite element calculation (one ABAQUS run). So there were a total of 203 runs. For each run, the mesh and/or boundary conditions had to be modified. Instead of using a commercial graphical mesh generator, a Fortran 90 program was written which reads a file containing the values of problem definition parameters and mesh definition parameters, and then generates an ABAQUS input file. This results in a consistent and precise method of mesh generation. For each specimen type (CCT or SENT), a particular mesh (node coordinates and element - node connections) was generated from the values of six parameters; the specimen width (w), the specimen height (h), the crack length to specimen width ratio (a/w), the number of element sectors (n_s), the number of element orbits (n_o), and the ratio of the specimen width to the radius of the inner element orbit (w/r_1). Figure 8 shows examples of the meshes that were used. The program attempts to make all of the element sector angles equal. The curve of the inner element orbit is always circular. Assume for each mesh that the origin of a coordinate system is located at the crack tip, the x axis is parallel to the crack with positive direction pointing toward the specimen's uncracked edge, and at the y axis is perpendicular to the crack with positive direction pointing towards the top of the mesh. Along each of the three axis sector lines ($+x$, $-x$, $+y$) the growth rate of the distances between adjacent element orbit lines (the orbit space growth rate) is constant. The growth rate along one of these sector lines is calculated from the sector line's length, the number of element orbits, and the radius of the inner element orbit (r_1). For all 203 runs, four of the six mesh parameters were constant, i.e., $w = 1$, $n_s = 48$, $n_0 = 48$, $w/r_1 = 1000$. h was varied according to the specimen aspect ratio (h/w), and (a/w) was also varied. This means that the same basic mesh was used for all 203 runs. ABAQUS input files could be quickly generated, and in one instance 77 were made within an hour. Eight node rectangular isoparametric plane stress elements were used with full integration. Each of the crack tip elements was made triangular by locating three nodes along one element side at the crack tip. All of the crack tip nodes were tied together. The side nodes of the crack tip elements were moved to the quarter points. 48 calculations of the J-integral were made for each ABAQUS run (each element orbit line was used for a contour). For almost every run, the J values varied for only a few of the innermost and outermost contours. Usually the J values for the bulk of a particular run's contours were identical to each other. It so happened that for the runs when $a/w = 0.01$, the orbit space growth rate along the $-x$ sector line (the crack sector line) was less than one. This is because $r_1 > a/48$, i.e., $w/1000 > 0.01w/48$. (This means that r_1 was bigger than the average of the 48 orbit spaces along the crack sector line (if r_1 equaled $a/48$, then the orbit space growth rate would equal one).) However, for these cases Table 1 seems to show that the calculated J values are still reasonable. Each SENT specimen mesh models one half of the symmetric specimen (dividing the specimen along the crack). Therefore, the aspect ratio for a SENT specimen mesh is equal to $h/(2w)$, i.e., it is one half of the aspect ratio for the corresponding SENT specimen (h/w). In Figure 8, all of the meshes are for SENT specimens, so the aspect ratio of each of the three shown meshes is equal to one half of the aspect ratio of the associated specimen.

In Figure 8, for each mesh the location of the crack tip is visible at the bottom, and the crack is along the bottom to the left of the crack tip. Each CCT mesh modeled one quarter of the bi-symmetric specimen (dividing the specimen along the crack and across the crack's midpoint). So the aspect ratio for a CCT specimen mesh is equal to the aspect ratio for the same CCT specimen. For both types of specimen meshes (CCT, SENT) the mesh bottom to the left of the crack tip (the crack) was subjected to a zero traction, and so was the right edge of the mesh. The mesh bottom to the right of the crack tip was constrained from movement in the y direction. The top of the mesh was constrained from movement in the x direction. The top of the mesh was either subjected to a uniform displacement or a uniform load in the y direction. For SENT specimen meshes, the left edge was subjected to a zero traction. For CCT specimen meshes, the left edge was constrained from movement in the x direction. Table 1 indicates that 25 of the 203 runs failed. All of the failed runs were for $a/w \le 0.10$. In these cases ABAQUS complained that some element areas were negative. It is unlikely that any element area was literally negative; i.e., it is unlikely that one part of an element's boundary crossed another part. "Negative" probably means a mathematically prohibited shape (For a simpler element, a four node rectangle, an example of a prohibited shape is when one of the interior angles is greater than π).

CONCLUSIONS

The specimen geometry stress intensity correction factor $F = \sqrt{JE}/(\sigma\sqrt{\pi a})$ is independent of specimen size (multiplying a, h, and w by the same scalar doesn't change F). F is dependent on specimen proportion $(a/w, h/w)$. For both types of specimens considered (CCT, SENT), for the boundary condition of prescribed uniform load, decreasing the specimen aspect ratio (h/w) increases F. For both types of specimens, for the boundary condition of prescribed uniform displacement, decreasing h/w decreases F. For any typical SENT specimen subjected to prescribed uniform displacement, the effect of h/w on F cannot be neglected, and for each set of geometry parameters $(a/w, h/w)$ a finite element calculation is required to determine F. For SENT specimens subjected to prescribed uniform load, the effect of h/w on F can be neglected, and equation (7) can be used to calculate F, when $h/w \ge 2$. For CCT specimens subjected to either prescribed uniform displacement or prescribed uniform load, the effect of h/w on F can be neglected, and equation (6) can be used to calculate F, when $h/w \ge 3$.

REFERENCES

1. T.L. Anderson, Fracture Mechanics, Fundamentals and Applications, 2nd edition, CRC Press, 1995, p. 63.

SPECIMEN*	a / w = 0.01	a / w = 0.05	a / w = 0.10	a / w = 0.20	a / w = 0.30	a / w = 0.40	a / w = 0.50
CCT EQ6	1.000	1.001	1.006	1.024	1.058	1.109	1.186
CCT L14	**	1.038	1.107	1.338	1.640	1.995	2.425
CCT L21	1.034	1.020	1.023	1.040	1.072	1.121	1.197
CCT L31	0.981	**	1.006	1.024	1.058	1.109	1.186
CCT L41	0.972	**	1.006	1.024	1.058	1.109	1.187
CCT L51	0.975	**	1.006	1.025	1.058	1.110	1.187
CCT L81	1.003	**	**	1.024	1.058	1.109	1.187
CCT D14	**	1.014	0.904	0.733	0.675	0.678	0.725
CCT D21	1.118	1.024	1.023	1.040	1.072	1.122	1.197
CCT D31	1.082	**	1.007	1.025	1.058	1.110	1.187
CCT D41	1.068	**	1.006	1.024	1.058	1.109	1.187
CCT D51	1.064	**	1.005	1.023	1.058	1.109	1.187
CCT D81	1.071	**	**	1.023	1.057	1.109	1.187
SENT EQ7	1.125	1.147	1.196	1.367	1.655	2.108	2.827
SENT L14	**	0.926	1.407	2.461	3.610	4.862	6.220
SENT L21	**	1.125	1.172	1.351	1.647	2.103	2.821
SENT L31	**	1.147	1.191	1.368	1.660	2.112	2.825
SENT L41	1.147	1.148	1.189	1.367	1.660	2.112	2.825
SENT L51	1.121	1.145	1.188	1.367	1.660	2.112	2.825
SENT L81	1.104	**	1.189	1.367	1.660	2.112	2.825
SENT D14	**	0.686	0.598	0.497	0.467	0.474	0.512
SENT D13	**	0.727	0.668	0.575	0.543	0.551	0.593
SENT D12	**	0.787	0.763	0.694	0.665	0.675	0.724
SENT D11	**	0.950	0.946	0.917	0.902	0.919	0.977
SENT D21	**	1.110	1.115	1.136	1.168	1.217	1.294
SENT D31	**	1.124	1.152	1.215	1.298	1.400	1.526
SENT D41	1.037	1.093	1.151	1.249	1.372	1.521	1.698
SENT D51	0.990	1.055	1.140	1.266	1.419	1.606	1.830
SENT D61	0.959	**	1.128	1.271	1.448	1.667	1.932
SENT D71	0.940	**	1.120	1.270	1.466	1.711	2.013
SENT D81	0.927	**	1.115	1.267	1.474	1.740	2.076

Table 1. Finite element values of the specimen geometry stress intensity correction factor, $\frac{\sqrt{JE}}{\sigma\sqrt{\pi a}}$.

* Each specimen is indicated by a type, either "CCT" or "SENT", an upper case letter, either "L" or "D", and a two digit number. "L" indicates that uniform load is prescribed. "D" indicates that uniform displacement is prescribed. The number indicates the specimen aspect ratio. For example, specimen "SENT D21" is a SENT specimen with prescribed uniform displacement, and $h/w = 2/1$.

** No value determined. ABAQUS error message said that some elements indicated negative areas for calculations at some integration points.

CCT EQ6 ==> Values for CCT specimen are calculated using equation 6. (No finite element calculations.)
SENT EQ7 ==> Values for SENT specimen are calculated using equation 7. (No finite element calculations.)

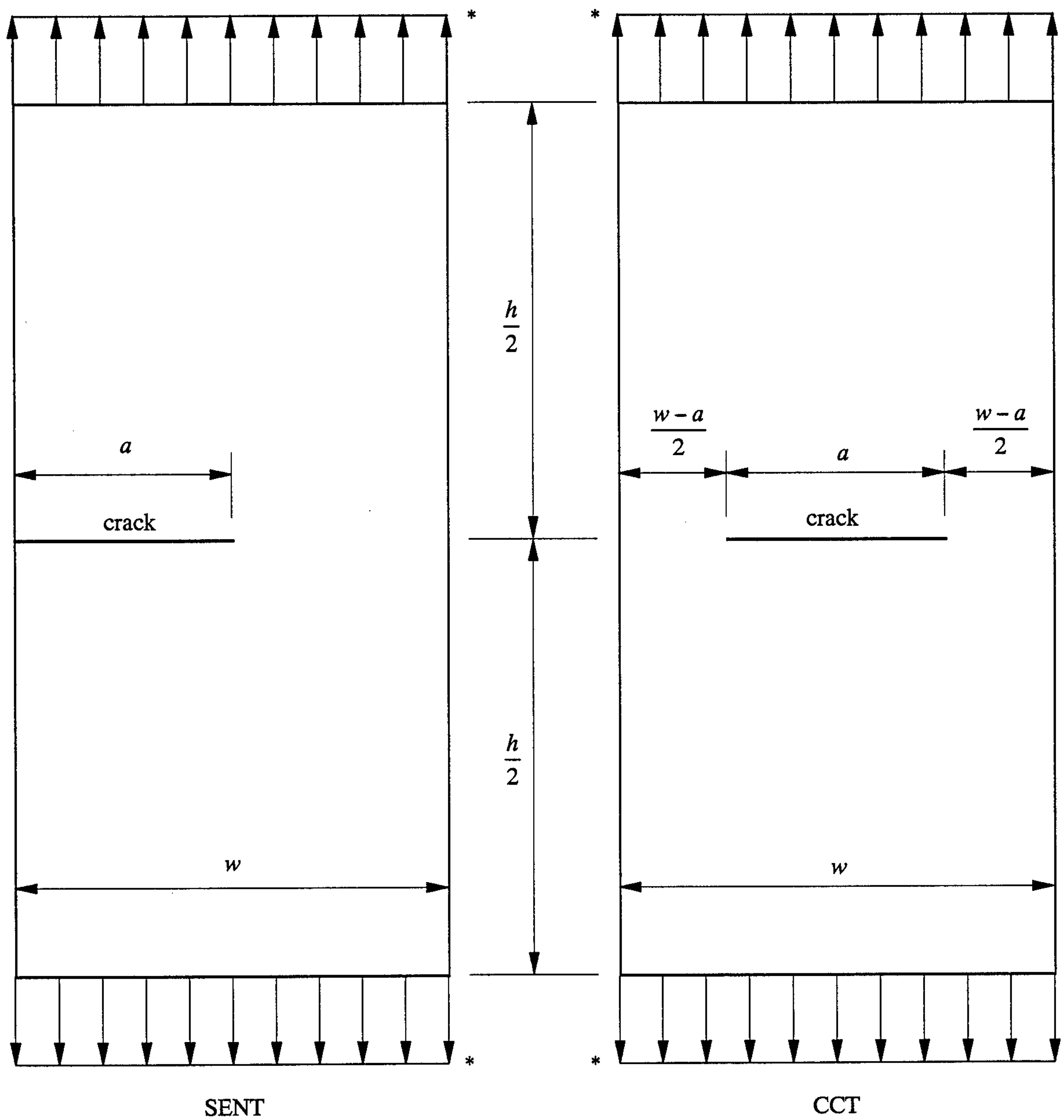

Figure 1. Specimen types

* Indicates prescribed quantity; prescribed uniform load, or prescribed uniform displacement.

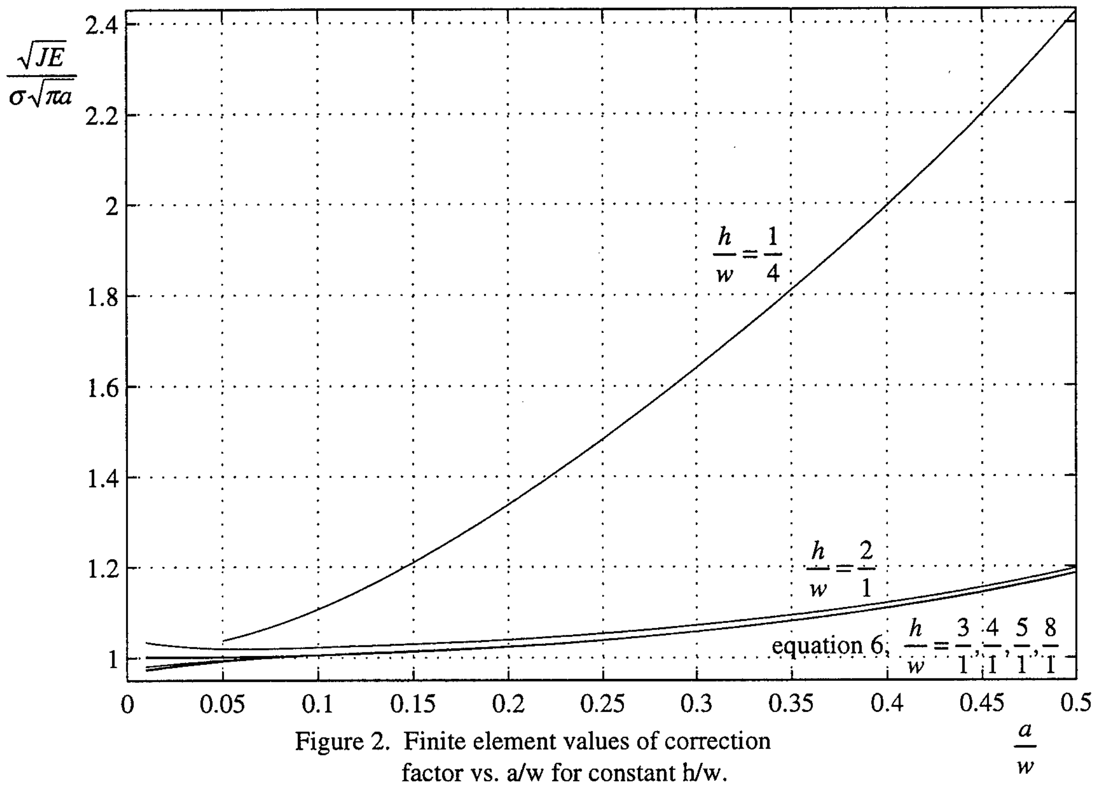

Figure 2. Finite element values of correction factor vs. a/w for constant h/w. CCT specimens with prescribed uniform load.

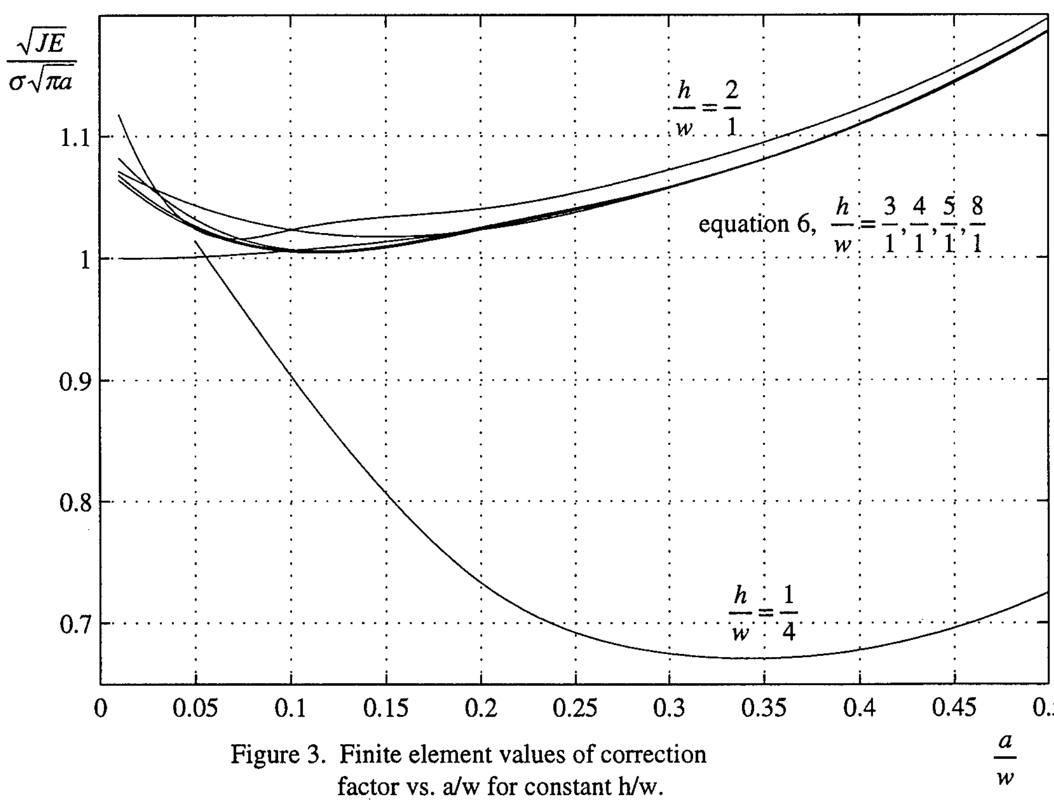

Figure 3. Finite element values of correction factor vs. a/w for constant h/w. CCT specimens with prescribed uniform displacement.

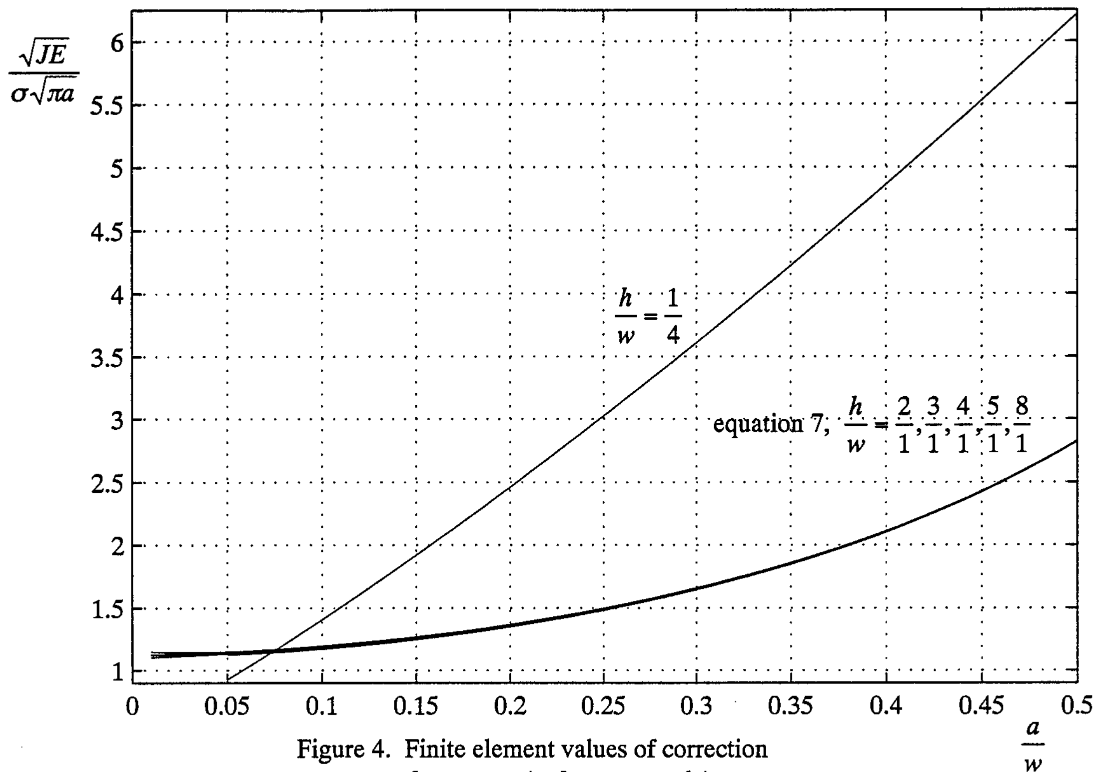

Figure 4. Finite element values of correction factor vs. a/w for constant h/w. SENT specimens with prescribed uniform load.

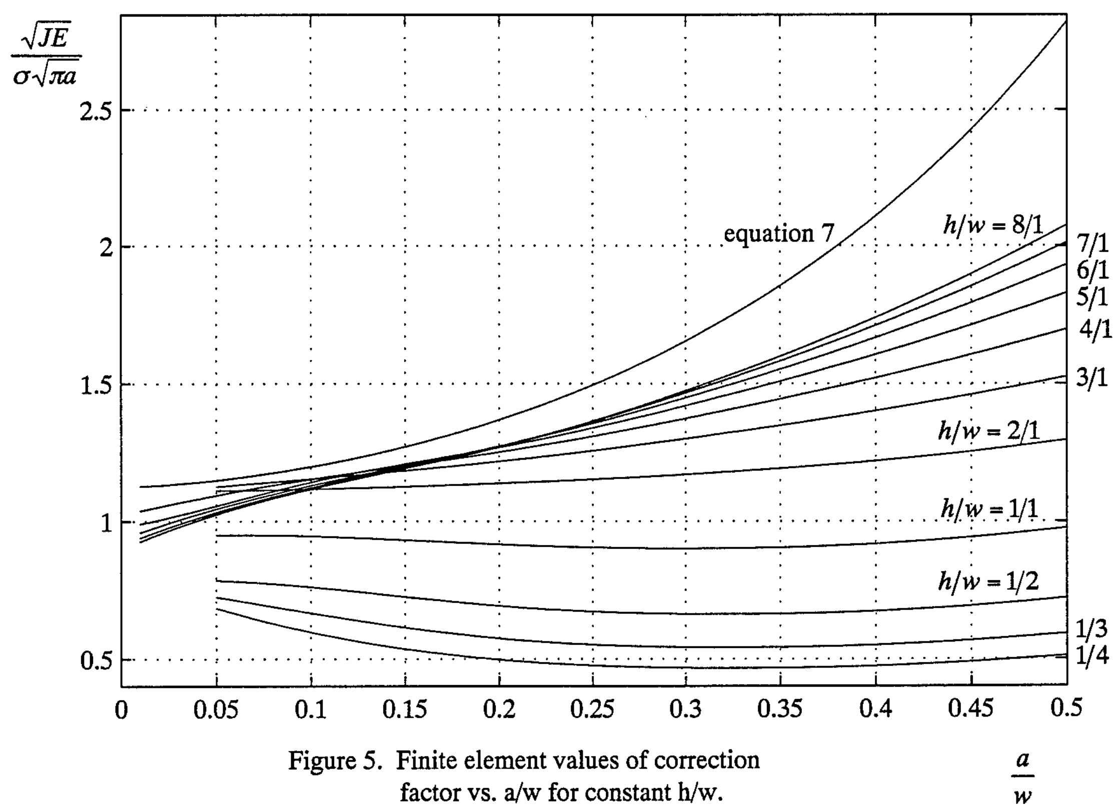

Figure 5. Finite element values of correction factor vs. a/w for constant h/w. SENT specimens with prescribed uniform displacement.

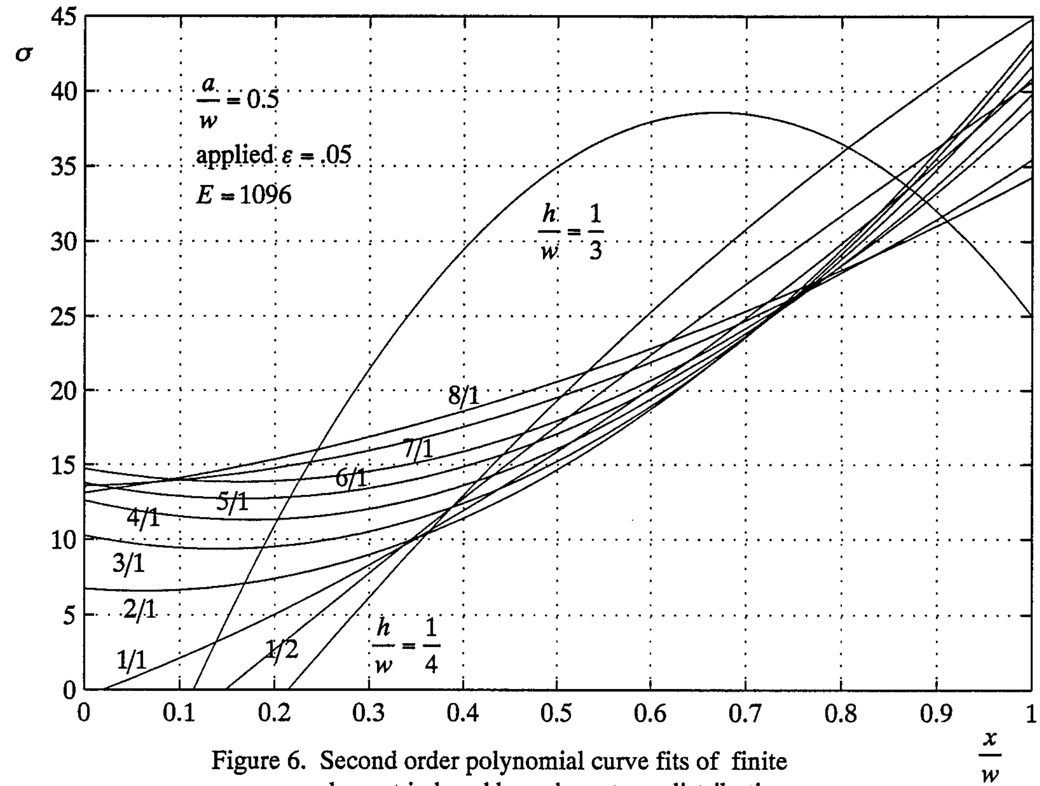

Figure 6. Second order polynomial curve fits of finite element induced boundary stress distributions. Constant h/w. SENT specimens with prescribed uniform displacement.

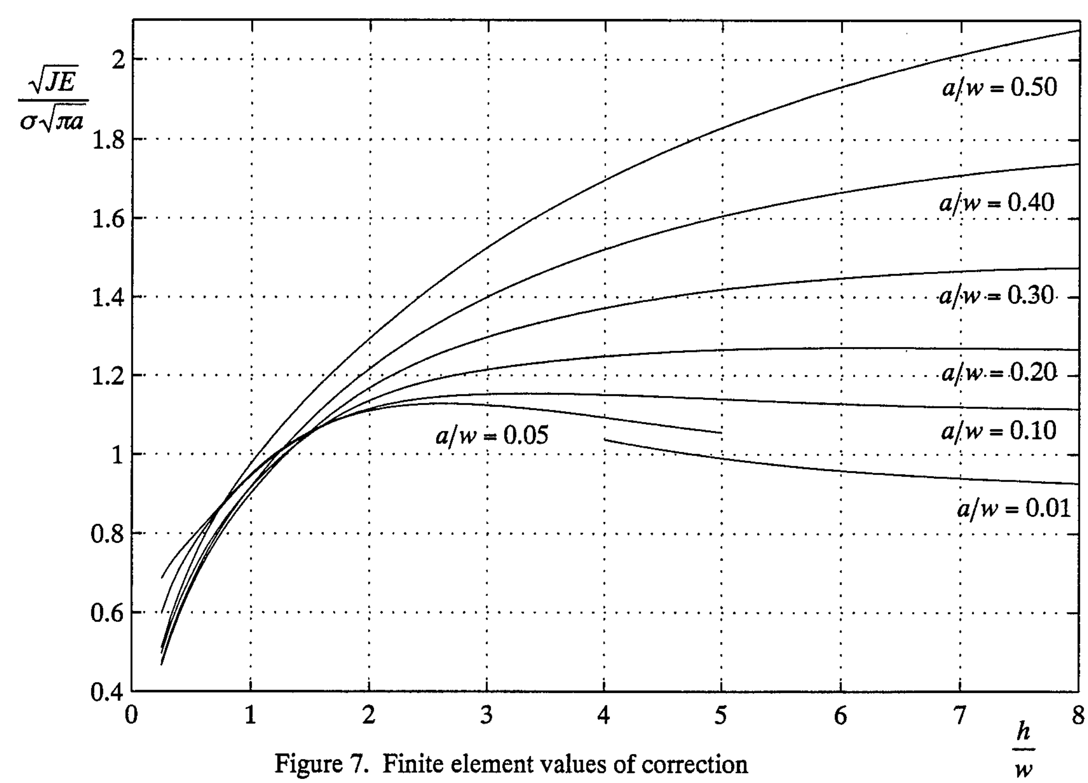

Figure 7. Finite element values of correction factor vs. h/w for constant a/w. SENT specimens with prescribed uniform displacement.

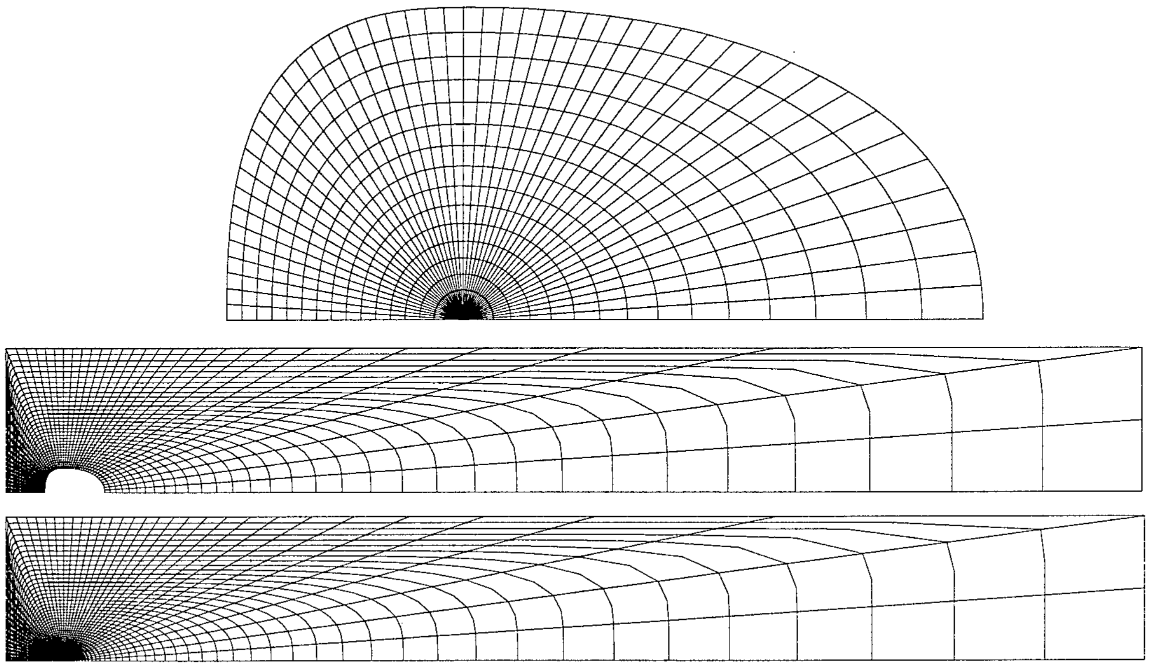

SENT mesh for h / w = 1 / 4; (a / w = 0.05) top: element orbits 1-16;
middle: element orbits 17-48; bottom: element orbits 1-48 (whole mesh)

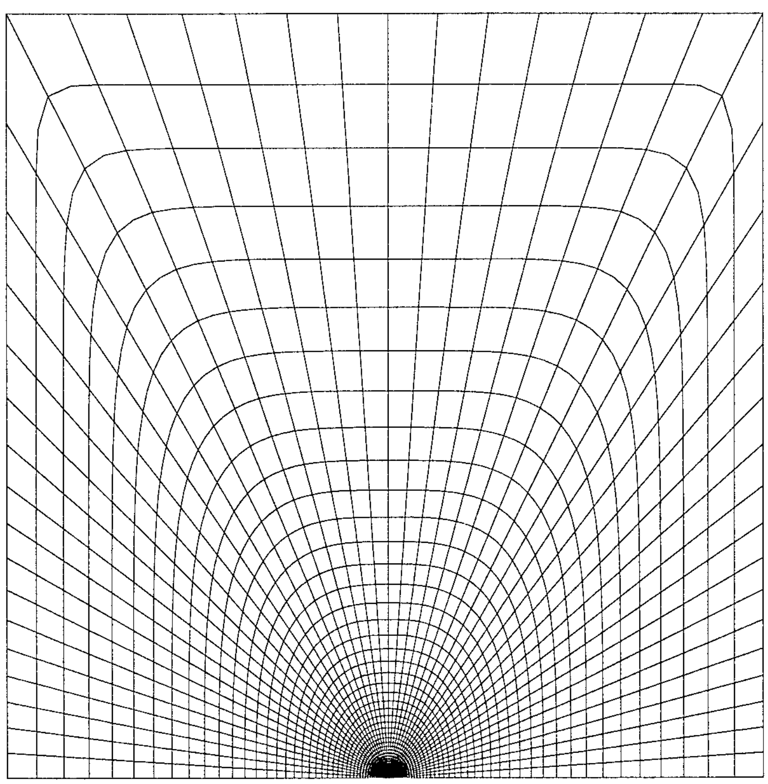

SENT mesh for h / w = 2 / 1
(a / w = 0.50)

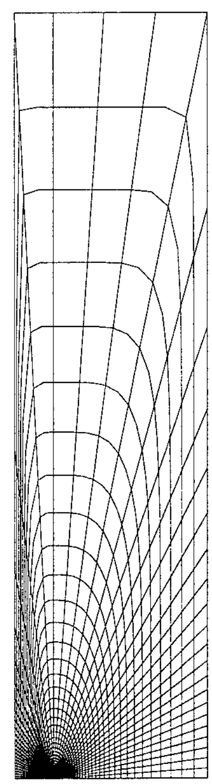

SENT mesh for h / w = 8 / 1
(a / w = 0.20)

Figure 8. Example finite element meshes